Renewable electricity storage using electrolysis

Zhifei Yan[a], Jeremy L. Hitt[a], John A. Turner[b,1], and Thomas E. Mallouk[a,1]

[a]Department of Chemistry, The University of Pennsylvania, Philadelphia, PA 19104; and [b]Private address, Broomfield, CO 80023

Edited by Richard Eisenberg, University of Rochester, Rochester, NY, and approved November 18, 2019 (received for review September 13, 2019)

Electrolysis converts electrical energy into chemical energy by storing electrons in the form of stable chemical bonds. The chemical energy can be used as a fuel or converted back to electricity when needed. Water electrolysis to hydrogen and oxygen is a well-established technology, whereas fundamental advances in CO_2 electrolysis are still needed to enable short-term and seasonal energy storage in the form of liquid fuels. This paper discusses the electrolytic reactions that can potentially enable renewable energy storage, including water, CO_2 and N_2 electrolysis. Recent progress and major obstacles associated with electrocatalysis and mass transfer management at a system level are reviewed. We conclude that knowledge and strategies are transferable between these different electrochemical technologies, although there are also unique complications that arise from the specifics of the reactions involved.

electrolysis | renewable energy | energy storage

Building sustainable, clean energy systems is one of the most critical problems that the world faces in this century. Population growth and economic development in the coming decades will inevitably result in a substantial increase in global energy consumption (1, 2). Traditional fossil sources of energy are carbon-positive and contribute substantially to climate change. Various alternative sources of carbon-neutral power exist, including nuclear fission, biofuels, and electricity generation from renewable resources such as wind and solar energy (1). It is projected that renewable electricity can provide a dramatic decrease in carbon dioxide intensity, defined as carbon dioxide emissions per unit of energy output, despite the projected increase in overall energy consumption (3).

Electricity from renewable sources such as wind and solar has become economically competitive due to years of cost decline and advances in technology. The globally averaged levelized cost of electricity (LCOE) for utility-scale solar photovoltaic (PV) power has fallen 73% since 2010, while the LCOE from onshore wind has reached $0.03kWh in some parts of the world (4). The price of renewable electricity from all currently commercial sources is projected to be comparable to or lower than that of fossil fuel-derived electricity by 2020 (4). One of the major contributors to the falling LCOE for solar and wind power electricity comes from the sharp reduction in installation costs. The global capacity weighted average total installation cost of newly commissioned utility-scale PV projects has decreased by 68% to around $1,600/kW since 2010. The construction costs of the new nuclear- and coal-fired power plants are very uncertain and are subject to various factors; however, total costs between $5,500 and $8,100/kW and $3,500/kW, respectively, have been suggested and are expected to increase in the future (5, 6).

Despite of the rapid growth of renewable electricity, the current fraction of power generated from renewable sources in the electric energy mix remains low, with a much greater proportion of electricity being produced from gas, oil, and coal. However, based on a reference case prediction, electricity from renewable resources is expected to increase from 18% to about 31% between 2018 and 2050 (3). One of the issues with solar electricity is the intermittent nature of the diurnal solar cycle, which is not well matched with demand and thus requires excess generation capacity at the grid level or backup power on the consumer end. For example, Fig. 1 shows the net electrical load fluctuation as a function of time for a spring day in California. Starting from around 4 PM a supply of an additional 13,000 MW of electricity from nonsolar resources such as natural gas and nuclear within 3 h is needed to replace the electricity shortfall of solar power (7).

The fluctuating power from solar and wind thus requires massive energy storage, both in the short and long terms. There are multiple ways that electrical energy can be stored including physical approaches such as pumped hydroelectric and compressed air energy storage; large-scale batteries such as lead-acid, lithium, sodium sulfur batteries, and flow batteries; and electrolysis, with pumped hydroelectric being the current leading technology in the energy storage sector (8). Most of these methods suffer from being only suitable for short-term storage or are limited by particular geographic requirements. Electrolysis stands out as a means of storing electric energy in the form of stable chemical bonds. The potentially enormous energy capacity, negligible self-discharge rate, existing infrastructure, and low capital cost of containing renewably generated carbon-based fuels make them ideal for seasonal storage, a feature that is highly desirable given the seasonality of renewable energy sources. The need for such a technology will be increasingly acute with the larger anticipated penetration of the low-cost renewable electricity into the power grid, as illustrated in Fig. 1.

While water electrolysis to hydrogen and oxygen is a well-established technology, an efficient and cost-effective means of storing electrical energy in the form of liquid fuels does not yet exist. In order for such a technology to become economically competitive with abundant fossil fuels, one has to start with very cheap electricity. A technoeconomic analysis of CO_2 electrolysis indicates that a renewable electricity price below $0.04/kWh will be needed for electrolysis-derived fuels to be competitive with fossil-derived fuels (9). This is a target that renewable electricity is well on its way to reaching based on the International Renewable Energy Agency renewable cost database (4).

In Fig. 1, we illustrate how a sustainable energy cycle can be achieved by coupling electrolysis with electricity generated from solar and wind, among other renewable sources. Electrolysis can produce both commodity chemicals and hydrogen, mitigating the intermittency of the renewable power. In this scenario, hydrogen-air fuel cells can be used to convert energy that is stored as hydrogen back to electricity. High-energy-density liquid fuels are the preferred form for seasonal storage and can form a green energy cycle if CO_2 in the air can be concentrated to enable efficient

This paper results from the Arthur M. Sackler Colloquium of the National Academy of Sciences, "Status and Challenges in Decarbonizing our Energy Landscape," held October 10–12, 2018, at the Arnold and Mabel Beckman Center of the National Academies of Sciences and Engineering in Irvine, CA. NAS colloquia began in 1991 and have been published in PNAS since 1995. From February 2001 through May 2019 colloquia were supported by a generous gift from The Dame Jillian and Dr. Arthur M. Sackler Foundation for the Arts, Sciences, & Humanities, in memory of Dame Sackler's husband, Arthur M. Sackler. The complete program and video recordings of most presentations are available on the NAS website at http://www.nasonline.org/decarbonizing.

Author contributions: J.A.T. and T.E.M. designed research; Z.Y. and J.L.H. performed research; and Z.Y., J.L.H., J.A.T., and T.E.M. wrote the paper.

The authors declare no competing interest.

This article is a PNAS Direct Submission.

[1]To whom correspondence may be addressed. Email: mallouk@sas.upenn.edu or h2wizard@gmail.com.

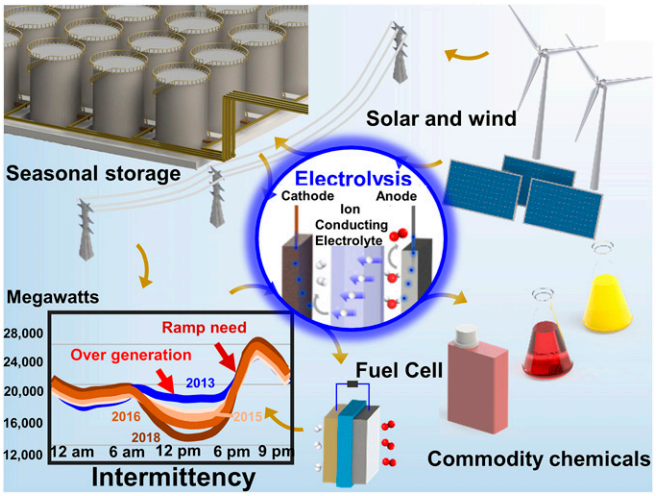

Fig. 1. Sustainable energy utilization. Schematics of energy storage and utilization based on electrolysis. Surplus electrical energy from renewable sources can be stored via electrolysis as chemical fuels. The energy is extracted to levelize demand on the short time scale and to meet the need for fuel in seasons when the renewable supply is less available. Intermittency plot (*Lower Left*) data from ref. 7.

electrolysis. There is growing research activity on the capture of carbon from the atmosphere (10), and a few companies are working to commercialize carbon capture technology. The electrolysis of CO_2 to CO and hydrogen (syngas) has been achieved with a variety of different electrocatalysts and provides a feedstock for hydrocarbon fuels via the Fischer–Tropsch process. Alternatively, C–C coupled products including ethylene and ethanol can be made directly by electrolysis at copper-containing catalysts, but the efficiency, selectivity, and throughput of those reactions need to be improved. Not shown in the figure is the electrochemical reduction of N_2 to ammonia for the production of fertilizers. In this case electrolysis takes advantage of an unlimited chemical feedstock as Earth's atmosphere provides the nitrogen and water needed for the reaction. In addition to making fuels and fertilizers by electrolysis, thermochemical catalysis provides an established method for hydrogenating CO_2, CO, and N_2. Two examples are the Fischer–Tropsch and Haber–Bosch processes, which are already well developed at scale for the production of liquid hydrocarbons and ammonia, respectively. It should be noted that nearly 80% of the energy consumed in ammonia synthesis is for hydrogen production via steam reforming and the water–gas shift reaction (11). Water electrolysis provides a potential carbon-neutral alternative for providing hydrogen for these reactions.

An electrolytic process is limited by 3 factors that act effectively as series impedances: electron transfer kinetics at the electrified interface, mass transport of reactants and products, and series resistance, including ion transport. Electron transfer across the electrified interface governs the kinetics of oxidation and reduction, and mass transport controls the availability of the reactant and the rate at which the product can be removed, as shown in Fig. 2*A*. The electron transfer rate and the mass transport flux are coupled as they both are proportional to the current. Active catalysts are needed to lower the activation barrier by binding and stabilizing certain transition states, Fig. 2*B*. Increasing the overpotential for one or both electrode processes accelerates the reaction kinetics by effectively lowering the activation barrier, but the extra energy cost lowers the power conversion efficiency, as illustrated in Fig. 2*D*. When the electron transfer kinetics are sufficiently fast, the highest current density is achieved by accelerating the supply of reactant. In the case of CO_2 electrolysis, this can be accomplished by supplying the reactant and removing the products in the gas phase, taking advantage of the faster diffusion coefficient of gases and avoiding the low solubility of CO_2 in liquid water, as shown in Fig. 2*C*.

Water Electrolysis

Water electrolysis has a long history, the first published demonstration dating to 1789, and it is now a well-established commercial technology. For example, a large installation of alkaline electrolyzers by Norsk Hydro (1948 to 1990) at a hydroelectric plant was capable of generating about 70,000 kg H_2/d (8). The largest wind-hydrogen plant was installed in Norway in 2004 by Norsk Hydro and Enercon, coupling a 600-kW wind turbine with a 48-kW electrolyzer (12).

There has been increasing interest in water electrolysis over the past 2 decades because of its potential role in a hydrogen-based energy economy involving electrolytic production, storage, transport, and use of hydrogen as fuel (2). Current research focuses on water electrolyzers that can be categorized according to their electrolytes: alkaline electrolytes, proton-exchange membranes (PEM), and solid-state proton or oxide ion conductors. Commercial PEM electrolyzers achieve the best performance (~70% energy efficiency at current densities of 1.7 A/cm^2, Giner Inc.) (13) but the large overpotential of the anodic water oxidation reaction and the corrosive acidic environment necessitate the use of precious metal catalysts. The membrane electrolyte and manufacture of the bipolar plates also add significantly to cost. Alkaline electrolyzers are the oldest technology with somewhat lower system efficiency (~64% efficiency, at current densities of 1 A/cm^2, GHW) and lower cost ($800/kW) (13). Alkaline electrolytes enable the use of nonprecious metal catalysts such as Ni and Fe.

There has been recent interest in developing better catalysts to lower the cost and increase the efficiency of water electrolysis. In acidic PEM electrolyzers, a volcano plot correlates the rate of the cathodic hydrogen evolution reaction (HER) with metal–hydrogen bond strength on various metal catalysts (Fig. 3*A*) (14). A simple explanation for the volcano shape is that metals that bind hydrogen too weakly cannot stabilize the M–H intermediate, whereas those that make very strong M–H bonds fill most of the binding sites, leaving little room for a new adsorption event. While the M–H bond strength is a good descriptor for most catalysts, some metals with particular facets, such as Pt (111), exhibit 20 to 200 times higher HER exchange current density in acid than in base, even though the H-binding energy is similar. Mechanistic

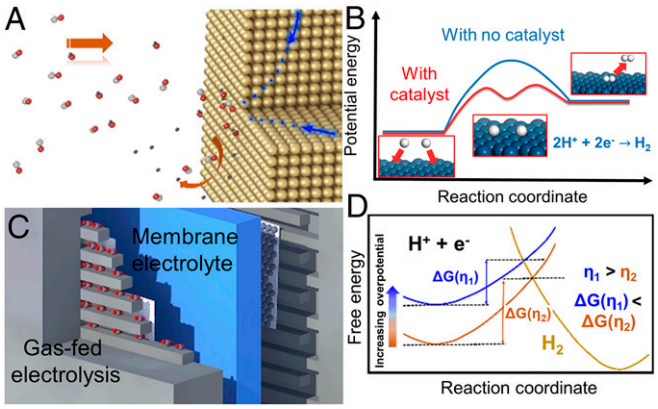

Fig. 2. Schematics of electrolysis. (*A*) Reactants transport to the surface of an electrode where a cathodic reaction occurs. (*B*) Comparison of the reaction pathways for the HER with and without catalyst. The catalyst stabilizes the intermediate and lowers the activation energy. (*C*) Electrolyzers in a gas-fed configuration. Gas-fed electrolysis exploits the fast diffusion of gaseous molecules, enabling high current density. Membrane electrolytes are usually required for ion management and gas separation. (*D*) Kinetics of the electrochemical HER. Transition state energy decreases as overpotential increases.

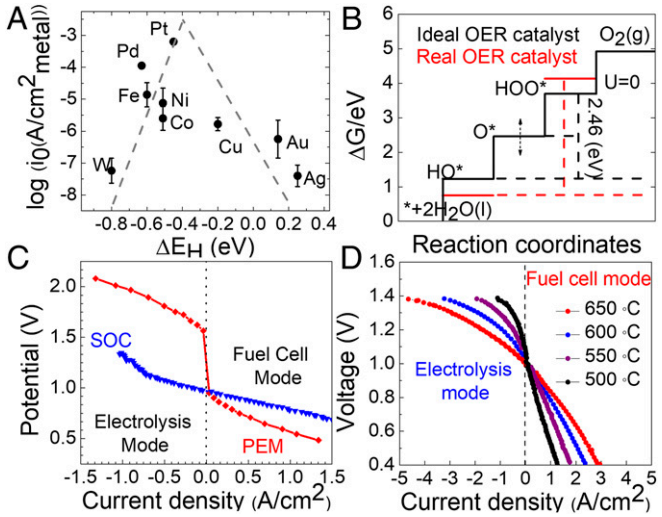

Fig. 3. Water electrolysis. (*A*) HER volcano plot for catalytic elements. Data from ref. 14. (*B*) Free energy diagram for the OER. The black curve refers to an ideal OER catalyst whereas the red curve represents a real catalyst (22). (*C*) Comparison between a low-temperature PEM electrolyzer and a higher-temperature SOEC. Data from ref. 43. (*D*) Electrolyzer and fuel cell mode performance of an SOEC using a proton conductor at intermediate temperatures. Increasing the temperature by 150 °C dramatically improved the cell current density. Data from ref. 44.

studies point to the role of hydroxide adsorption (15) or water reorganization under the interfacial electric field during the HER process (16). Precious metals (Pd and Pt) are the best catalysts but their cost and low natural abundance present obstacles to use of this technology on a very large scale. Thus, an appealing strategy is to replace pure Pt with core-shell, over-, and sublayer, doped and supported structures. Further reduction in precious metal loading is possible by using single-atom catalysts, which have emerged in the recent few years. The high surface energy of single atoms favors their coalescence and requires supports that can anchor them strongly. Electrocatalyst supports can also stabilize catalytic metal atoms and modulate their reactivity by donating or accepting electrons. For instance, there is evidence of d-electron transfer between late transition metal (oxide) and early transition metal layered supports in the strong metal–support interaction (17). Similar considerations may be applicable to alloys containing metals with different electron negativities.

One of the important factors in electrocatalysis is the catalytically active surface area. Current density normalized to the active surface area often reveals site turnover rates and activation energies similar to the planar counterpart, even though the current can differ by orders of magnitude (18). However, uncertainties can arise in surface area measurements from experimental conditions, including electrolyte conductivity, surface coverage, and time scales (19). Also, because the electron transfer kinetics are fast in acidic aqueous electrolytes, HER activity is typically mass transfer-limited and requires forced convection or ultramicroelectrode techniques to measure its intrinsic activity.

Recently, a number of nonprecious-metal HER catalysts have been discovered. Inspired by the MoFe cofactor of nitrogenase, which has a hydrogen binding energy close to that of Pt, the edge sites of MoS_2 as well as several metal phosphide catalysts have been shown to be active toward HER (20). Recent studies have shown that S vacancies and strain engineering are also effective ways to improve HER performance (21).

The 4-electron, 4-proton oxygen evolution reaction (OER) is more mechanistically complex and invariably involves substantial (250 to 300 mV) onset overpotentials in acidic media. The reaction is thought to proceed via an adsorbed M–OH species, followed by a deprotonation step. Oxygen gas is formed either from a surface hydroperoxy intermediate, M–OOH, or by bimolecular recombination of M–O. For oxide-based OER catalysts with rocksalt, rutile, spinel, and perovskite structures, volcano plots have been developed from theoretical considerations (22). An ideal OER with optimal binding energies has a free energy difference between M–OOH and M–OH $(\Delta G_{OH} - \Delta G_{OOH})$ of 2.46 eV, requiring an onset potential of 1.23 V (Fig. 3*B*). Onset potentials of real catalysts, however, are significantly higher because $(\Delta G_{OH} - \Delta G_{OOH})$ deviates from the ideal case and is proposed to be regulated by the free energy of M–O bonding. A universal average $(\Delta G_{OH} - \Delta G_{OOH})$ value of 3.2 eV is consistent with several groups of catalysts because the binding strength of OH scales linearly with that of OOH (22). Although the scaling relation is a useful concept in understanding catalytic activity, experimental quantification is complicated by the fact that the properties of catalyst surfaces may change during electrochemical operation, particularly under anodic conditions. Metal oxidation states, for example, vary with the applied potential, and this effect can lead to dramatic changes in catalytic activity, conductivity, and stability. The transition from Ni^{2+} to Ni^{3+} is typically a prerequisite for high OER activity in alkaline nickel-based catalysts as the former is insulating. Pretreatment of the catalyst surface before testing is important for meaningful evaluation and comparisons. Metal oxides with high solubility at higher oxidation states are often unstable in acid media and a trade-off between the stability and activity of Pt, Pd, Au, and Ru has been observed (23). Currently, iridium oxide is the only known stable catalyst for oxygen evolution in acidic media, and it is used only in pure form in the catalyst layer.

Conductive supports can be used to reduce the precious metal loadings, leading to lower costs and a better utilization of catalysts. However, while carbon can be used as a conductive support for both half-reactions in a fuel cell, it can only be used on the hydrogen side in a PEM electrolyzer; on the oxygen side it quickly corrodes. Oxide supports such as mesoporous tin oxide doped with indium have shown high conductivity (0.3 S/cm) and promising electrochemical stability at anodic potentials (24). Two of the key research topics for acid electrolysis are thus finding a more abundant, lower-cost alternative catalyst to iridium oxide for oxygen evolution and/or discovering a conductive support that also has long-term stability under oxygen evolution conditions in acidic media.

CO_2 Electrolysis

Electrochemical reduction of CO_2 to liquid fuel and value-added chemicals represents a possible solution for carbon-neutral seasonal storage of renewable electricity. CO_2 can be reduced to various C1 products including carbon monoxide (CO), formate, methane, methanol, and C2+ products including ethylene and ethanol (25). CO_2 reduction with high selectivity to CO and formate has already been realized since these reactions are a 2-electron transfer process (26). It is more challenging to obtain a C2+ product with high selectivity as the process requires transferring more than 2 electrons and multiple protons, thus requiring multiple reaction intermediates, some of which are shared with different possible products. The high overpotential required for most CO_2 reduction catalysts also implies a low energy conversion efficiency, <50% (compared to the 60 to 70% for water electrolyzers) (9).

As discussed for the OER, the efficiency of CO_2 reduction on metallic catalysts is limited by linear scaling relations. For example, Fig. 4*A* plots a correlation of the free energy (calculated by density functional theory, DFT) of 2 intermediates in the reduction of CO_2 to CO, E(COOH), and E(CO). A lower free energy and more stable M–COOH bond is desired, whereas weaker binding to CO is necessary to optimize desorption of the product (27). This is challenging for a single metal catalyst if the intermediates bind to the same site because the M–C bond strengths scale linearly. Multimetallic catalysts take inspiration from the active site of the

CO dehydrogenase enzyme CODH, in which cooperative binding to 2 metal atoms stabilizes a CO_2^- transition state (28, 29). Cu is a unique CO_2 reduction catalyst because it favors C2+ products, including some like ethanol that are ideal for seasonal storage. Cu makes a moderately strong bond to CO but not so strong as to poison the surface, allowing sufficient coverage for C–C coupling or protonation steps (30, 31). The catalytic pathways leading to hydrocarbons or oxygenates on Cu are complicated and highly coupled, as evidenced by the relatively low Faradaic efficiency (FE) for producing ethylene and ethanol (Fig. 4*B*). Alloying Cu with other metals (29, 32–34) and building nanostructures that modulate the chemical environment of the CO binding site (35–37) are interesting strategies for steering the C2+ product distribution. Given the complexity of this problem, there is a need for better spectroscopic probes and microscopies that can characterize the structure of the electrocatalytic sites. Systematic high-throughput screening guided by computation and machine learning are also emerging as effective means of attacking electrocatalytic problems of this nature (38).

There are also acute system-level problems for CO_2 electrolysis. The low solubility of CO_2 in water under acidic conditions creates a mass transfer limitation, and at high overpotentials the HER reaction becomes dominant. Strategies for concentrating CO_2 at the electrode surface can mitigate this problem to a certain extent (Fig. 4*C*) (39) and mass transfer is dramatically improved when CO_2 is supplied in the gas phase. In this case, construction of a high-surface-area triple-phase boundary (TPB) where catalyst, electrolyte, and gaseous reactant meet is essential. Fig. 4*D* shows a TPB made by sputtering a Cu catalyst layer onto a polytetrafluoroethylene (PTFE) substrate that prevents system flooding, on top of which is deposited a carbon conductive layer. Gaseous CO_2 diffuses through the porous PTFE layer and the HER is suppressed by using an alkaline electrolyte (40). Lessons from biological systems such as the C4 plants (plants with alternative photosynthetic pathway incorporating CO_2 into a C4 intermediate, oxaloacetate) may inspire other strategies for concentrating CO_2 in a TPB configuration. Photosynthetic organisms have evolved the ability to channel CO_2 to ribulose-1,5-bisphosphate as carbon source for the Calvin cycle. C4 plants acquire extra concentration by trapping CO_2 in a 4-carbon compound and passing it to bundle sheath cells for decarboxylation, resulting in a local supply of CO_2 for fixation (41). Analogous CO_2 storage and delivery would be addressing a major problem of gas-fed CO_2 electrolyzers, because the single-pass conversion rate in current electrolyzers is low. One can imagine equipping the diffusion layer in an electrolyzer with gradient-localized "bundle sheath cells" that salvage the unreacted CO_2 gas from the TPB and pass it down to reactive sites, achieving higher conversion rates.

A number of lessons learned from water electrolyzers can be applied to the CO_2 electrolysis problem, although some problems are CO_2-specific. pH gradients developed across the membrane electrolyte cost energy in water electrolyzers that operate in neutral or near-neutral solution, and for this reason all water electrolyzers operate under strongly acidic or strongly basic conditions. The use of buffered solutions in CO_2 electrolysis creates pH gradients and proton management problems at high current density. For water electrolyzers, a bipolar membrane (BPM) addresses this problem by operating the cathode and anode in acid and base, respectively. This arrangement minimizes the membrane polarization loss because water autodissociation in the BPM provides H^+ and OH^- ions to the cathode and anode, respectively. This strategy can be applied to CO_2 electrolysis, but with some modification since CO_2 reduction requires a different optimal pH from the HER. The use of BPM also mitigates the cross-over problem of both anionic and neutral products (42).

Solid-State Electrolytes

Because chemical reaction rates rise exponentially with temperature, intermediate- and high-temperature electrolyzers are

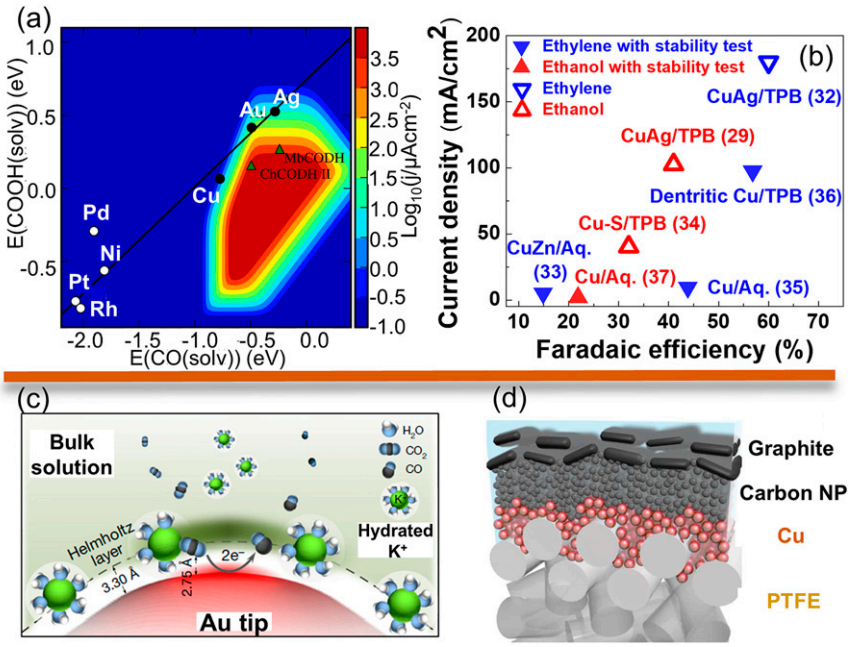

Fig. 4. CO_2 electrolysis. (*A*) The scaling relation between the adsorption strength of COOH and CO on various metal surfaces and in enzymes. Reprinted with permission from ref. 27. Copyright 2013 American Chemical Society. (*B*) Comparison of current density and FE of CO_2 reduction to ethylene (blue) and ethanol (red). Solid symbols refer to published stability tests. Higher current density is achieved in a triple phase boundary (TPB) configuration, compared to aqueous phase CO_2 reduction (Aq.). Data from refs. 29, 32–34, and 35–37. (*C*) Enhanced mass transfer of CO_2 near an Au needle surface. The large electric field at the tip of the Au needle attracts hydrated K^+, which concentrates CO_2 in its solvation shell. Adapted with permission from ref. 39, Springer Nature: *Nature*, copyright 2016. (*D*) Construction of the TPB in gas-fed CO_2 electrolysis. The Cu catalyst is sputtered onto a PTFE porous support, which provide a gas diffusion pathway. From ref. 40. Reprinted with permission from AAAS.

effective in lowering electrode overpotentials for both the anode and cathode reactions. Fig. 3*C* compares the polarization curves of PEM cell at 60 °C with a solid oxide electrolysis cell (SOEC) at 800 °C (43), and Fig. 3*D* shows data from a cell containing a solid-state proton conducting electrolyte (44). The electrode reactions in intermediate- (250 to 500 °C) and high-temperature (600 to 800 °C) electrolyzers are slightly different from those in polymer electrolyzers depending on the type of electrolyte used. For example, in an SOEC, water vapor or CO_2 is reacted at the cathode to produce H_2 or CO, respectively, and O^{2-} in a 2-electron process. At the anode, O^{2-} ions combine to form O_2 gas.

$(La_{1-x}Sr_x)_{1-y}MnO_3$ is one of the best studied catalysts for the SOEC anode but has trouble with delamination from the electrolyte, causing an increase in polarization (45). At the cathode, nickel and other late-transition metals are frequently used as SOEC catalysts but usually are not very stable at the temperatures required (46). Tests have been done using perovskites including $La_{0.6}Sr_{0.4}VO_{3-d}$ and $(La_{0.75}Sr_{0.25})_{0.95}Mn_{0.5}Cr_{0.5}O_3$ as catalysts at the cathode as well with promising results (47, 48). $La_{1-x}Sr_xGa_{1-y}Mg_yO_3$ has oxide ion conductivity 5 times higher than typical zirconia electrolytes, but its stability in an SOEC has not been studied in detail yet (49). One study using $La_{1-x}Sr_xGa_{1-y}Mg_yO_3$ in a solid oxide fuel cell found the output voltage to decay at 1 mV/h (50), which is not viable for a commercial system. Proton-conducting electrolytes are also very promising because they can achieve higher conductivity than oxyide-conducting materials at relatively low temperatures (51). The most studied type of proton-conducting electrolytes are $BaZrO_3$ and $BaCeO_3$ perovskites, where the former is more stable and the latter more conductive (52). A nice compromise between the 2 came from combining them to make $BaCe_{0.5}Zr_{0.3}Y_{0.2}O_{3-d}$, which resulted in an impressive 830 mA/cm^2 current density at 1.5 V (53). The downside to ceramic proton or oxide ion conductors is that the ion conductivities are not as high as polymer electrolytes and the high operating temperatures cause even the electrode and electrolyte materials to degrade over time. One way that researchers have tried to minimize the degradation is to lower the temperature of operation. Recently, solid acids have been shown to be good proton conductors at intermediate temperatures. For example, $CsHSO_4$, CsH_2PO_4, and $Cs_2(HSO_4)(H_2PO_4)$ have shown high proton conductivity as well as a few others including $Rb_3H(SeO_2)_2$, $(NH_4)_3H(SO_4)_2$, and $K_3H(SO_4)_2$. These materials achieve conductivities at temperatures as low as 120 to 300 °C but are limited by their brittle mechanical properties (54). Future research should focus on improving how the electrolyte and catalyst interface is made to minimize delamination. Another interesting development has been to use electrolytes that can conduct both protons and oxide ions. One group made a hybrid SOEC, using $BaZr_{0.1}Ce_{0.7}Y_{0.1}Yb_{0.1}O_{3-d}$ as the electrolyte, that could produce 3.16 A/cm^2 at 1.3 V and 750 °C. This performance is much better than that reported for single ion-conducting electrolytes (55). Research on solid-state systems for both water splitting and CO_2 electrolysis is showing steady progress and is promising for the generation of fuel and chemical feedstocks (H_2 and CO) from electrical energy. Haldor Topsøe already produces SOECs for large scale, on-demand CO production from CO_2 with purities as high as 99.999% (56).

Electrochemical Nitrogen Reduction

The electrosynthesis of ammonia (ESA) is being studied to better understand electrocatalytic activation of dinitrogen and its limitations. This has been done at a range of temperatures by reacting N_2 gas at a cathode and water at an anode that are separated by a proton-conducting electrolyte or reacting both N_2 and water at the cathode using an anion-conducting electrolyte. Because of the 6-electron nature of the N_2 reduction reaction, the Faradaic and energy efficiencies for combining water oxidation and nitrogen reduction tend to be very low. A more commonly studied approach is to use higher temperatures and feed H_2 to the anode. This can increase the FE at the cost of oxidizing the H_2 but high temperatures risk decomposing any NH_3 formed (57). In low-temperature ESA the most commonly studied membrane is Nafion because of its high conductivity and stability, although one of the highest FEs so far reported (41%) came from anion exchange polymer membrane with an iron cathode (58). Other catalysts tested include Pt, Ru, and conducting metal oxides with similar results (59). Several attempts to use molten salts at 400 °C with N^{3-} as mobile ion in the electrolyte and Ni as the catalysts reported FE as high as 80% and a synthesis rate faster than any solid oxide conductor (60). In this case, the electrocatalysts are typically late-transition metals such as silver, nickel, or palladium and the electrolytes are often the same as those used in water-splitting SOECs (59). One research group also used CH_4 as a hydrogen source instead of H_2 with similar results (61). Low FE and low current density are persistent challenges for ESA research. At higher temperatures, the FE ranges from <1 to 80% but the current densities are too low for practical purposes, ranging from <1 to 23 mA/cm^2. For temperatures below 100 °C, the FE is typically only 1 to 2%, although there are a few reports that have been considerably higher and may show promise if the current density can be improved (58). DFT calculations have helped to clarify the challenges in nitrogen electrocatalysis. Most notably, one group found that the differences in adsorption energies for NH_x* intermediates are far from the optimal values for the desired reaction, which presents a difficult challenge for ESA (62).

Outlook

The growth in renewable energy capacity from solar, wind, and other carbon-neutral sources is limited by the lack of adequate solutions for short- and long-term energy storage. Carbon-based liquid fuels are ideal for long-term energy storage because of their high energy density and the well-developed infrastructure for their transport, storage, and use. Electrolysis provides a key link between electrical energy and liquid fuel, either by direct electrosynthesis from CO_2 and water or through the generation of feedstocks for fuel synthesis, such as hydrogen and syngas. The latter electrolytic processes, which involve 2-electron, 2-proton cathode reactions, are already well-developed from the scientific and technological point of view. Water electrolysis using alkaline electrolyzers has been commercialized in parts of the world where hydroelectric power is cheap and abundant. Technology demonstrations for the production of CO and syngas have been successful with both low-temperature polymer electrolyte-based systems and high-temperature solid-state electrolyzers.

The direct electrolytic production of liquid fuels such as ethanol or ammonia requires us to master electrocatalytic reaction cascades beyond simple one-electron intermediates. While the reduction of CO_2 to C–C coupled products on copper-containing catalysts has been known since the 1980s, the detailed mechanism has only recently been understood by combining electronic structure theory with experimental electrochemical and spectroscopic experiments. Encouraging progress has been made in the search for catalysts and electrolytes that enable the selective production of C_2 products such as ethylene and ethanol, but high cathode and anode overpotentials limit the efficiency of these processes. In addition to the study of catalysis, strategies for improving the transport of reactants, products, and ions are also important for the development of efficient electrolyzers for CO_2 and N_2.

Our understanding of well-developed technologies such as water electrolysis provides a useful guide for other problems in electrochemical energy conversion. The principles of catalysis in multi-electron reactions, for example linear scaling relations, are transferable from one reaction to another. Lessons at the system level are also common to different electrolytic systems. For example, proton management using BPMs addresses system-level issues for both water and CO_2 electrolysis. The lowering of electrode overpotentials

at elevated temperatures is effective for water and CO_2 electrolysis to produce H_2 and CO and might in the future be applied to reactions that directly produce liquid fuel. Natural enzymatic systems also provide inspiration to develop new strategies for preconcentrating and delivering reactants and also controlling the environment of catalytically active sites to improve both the selectivity and efficiency of electrocatalysts for the production of liquid fuels.

Data Availability Statement

There are no data associated with this article.

ACKNOWLEDGMENTS. The authors acknowledge the Office of Basic Energy Sciences, Division of Chemical Sciences, Geosciences, and Energy Biosciences, Department of Energy for support of their research on solar photoelectrochemistry under contract DE-FG02- 07ER15911 and the Canadian Institute for Advanced Research Bio-Inspired Solar Energy program for support of their work on CO_2 electrocatalysis.

1. S. Chu, A. Majumdar, Opportunities and challenges for a sustainable energy future. *Nature* **488**, 294–303 (2012).
2. J. A. Turner, Sustainable hydrogen production. *Science* **305**, 972–974 (2004).
3. "Annual Energy Outlook 2019 with projections to 2050" (US Energy Information Administration, Washington, DC, 2019).
4. IRENA, "Renewable power generation costs in 2017" (International Renewable Energy Agency, Abu Dhabi, 2017).
5. D. Schlissel, A. Smith, R. Wilson, "Coal-fired power plant construction costs" (Synapse Energy Economics, Inc., 2018).
6. D. Schlissel, B. Biewald, "Nuclear power plant construction costs" (Synapse Energy Economics, Inc., 2008).
7. CAISO, "What the duck curve tells us about managing a green grid" (2013). https://www.caiso.com/Documents/FlexibleResourcesHelpRenewables_FastFacts.pdf. Accessed 8 September 2019.
8. M. Beaudin, H. Zareipour, A. Schellenberglabe, W. Rosehart, Energy storage for mitigating the variability of renewable electricity sources: An updated review. *Energy Sustain. Dev.* **14**, 302–314 (2010).
9. P. De Luna *et al*., What would it take for renewably powered electrosynthesis to displace petrochemical processes? *Science* **364**, eaav3506 (2019).
10. T. M. McDonald *et al*., Cooperative insertion of CO_2 in diamine-appended metal-organic frameworks. *Nature* **519**, 303–308 (2015).
11. I. Rafiqul, C. Weber, B. Lehmann, A. Voss, Energy efficiency improvements in ammonia production—Perspectives and uncertainties. *Energy* **30**, 2487–2504 (2005).
12. M. Korpås, C. J. Greiner, Opportunities for hydrogen production in connection with wind power in weak grids. *Renew. Energy* **33**, 1199–1208 (2008).
13. A. Buttler, H. Spliethoff, Current status of water electrolysis for energy storage, grid balancing and sector coupling via power-to-gas and power-to-liquids: A review. *Renew. Sustain. Energy Rev.* **82**, 2440–2454 (2018).
14. W. Sheng, M. Myint, J. G. Chen, Y. Yan, Correlating the hydrogen evolution reaction activity in alkaline electrolytes with the hydrogen binding energy on monometallic surfaces. *Energy Environ. Sci.* **6**, 1509–1512 (2013).
15. D. Strmcnik *et al*., Improving the hydrogen oxidation reaction rate by promotion of hydroxyl adsorption. *Nat. Chem.* **5**, 300–306 (2013).
16. I. Ledezma-Yanez *et al*., Interfacial water reorganization as a pH-dependent descriptor of the hydrogen evolution rate on platinum electrodes. *Nat. Energy* **2**, 17031 (2017).
17. M. E. Strayer *et al*., Charge transfer stabilization of late transition metal oxide nanoparticles on a layered niobate support. *J. Am. Chem. Soc.* **137**, 16216–16224 (2015).
18. L. Chen, Study of the kinetics of hydrogen evolution reaction on nickel-zinc alloy electrodes. *J. Electrochem. Soc.* **138**, 3321–3328 (1991).
19. C. Fan, D. L. Piron, P. Paradis, Hydrogen evolution on electrodeposited nickel-cobalt-molybdenum in alkaline water electrolysis. *Electrochim. Acta* **39**, 2715–2722 (1994).
20. E. J. Popczun *et al*., Nanostructured nickel phosphide as an electrocatalyst for the hydrogen evolution reaction. *J. Am. Chem. Soc.* **135**, 9267–9270 (2013).
21. H. Li *et al*., Corrigendum: Activating and optimizing MoS2 basal planes for hydrogen evolution through the formation of strained sulphur vacancies. *Nat. Mater.* **15**, 364 (2016).
22. I. C. Man *et al*., Universality in oxygen evolution electrocatalysis on oxide surfaces. *ChemCatChem* **3**, 1159–1165 (2011).
23. S. Cherevko *et al*., Dissolution of noble metals during oxygen evolution in acidic media. *ChemCatChem* **6**, 2219–2223 (2014).
24. H.-S. Oh, H. N. Nong, P. Strasser, Preparation of mesoporous Sb-, F-, and in-doped SnO_2 bulk powder with high surface area for use as catalyst supports in electrolytic cells. *Adv. Funct. Mater.* **25**, 1074–1081 (2015).
25. Y. Hori, "Electrochemical CO2 reduction on metal electrodes" in *Modern Aspects of Electrochemistry*, C. G. Vayenas, R. E. White, M. E. Gamboa-Aldeco, Eds. (Springer, New York, 2008), pp. 89–189.
26. Z. Liu, H. Yang, R. Kutz, R. I. Masel, CO_2 electrolysis to CO and O_2 at high selectivity, stability and efficiency using sustainion membranes. *J. Electrochem. Soc.* **165**, J3371–J3377 (2018).
27. H. A. Hansen, J. B. Varley, A. A. Peterson, J. K. Nørskov, Understanding trends in the electrocatalytic activity of metals and enzymes for CO_2 reduction to CO. *J. Phys. Chem. Lett.* **4**, 388–392 (2013).
28. D. Kim *et al*., Electrochemical activation of CO_2 through atomic ordering transformations of AuCu nanoparticles. *J. Am. Chem. Soc.* **139**, 8329–8336 (2017).
29. Y. C. Li *et al*., Binding site diversity promotes CO_2 electroreduction to ethanol. *J. Am. Chem. Soc.* **141**, 8584–8591 (2019).
30. A. A. Peterson, F. Abild-Pedersen, F. Studt, J. Rossmeisl, J. K. Nørskov, How copper catalyzes the electroreduction of carbon dioxide into hydrocarbon fuels. *Energy Environ. Sci.* **3**, 1311–1315 (2010).
31. R. Kortlever, J. Shen, K. J. P. Schouten, F. Calle-Vallejo, M. T. M. Koper, Catalysts and reaction pathways for the electrochemical reduction of carbon dioxide. *J. Phys. Chem. Lett.* **6**, 4073–4082 (2015).
32. T. T. H. Hoang *et al*., Nanoporous copper-silver alloys by additive-controlled electrodeposition for the selective electroreduction of CO_2 to ethylene and ethanol. *J. Am. Chem. Soc.* **140**, 5791–5797 (2018).
33. D. Ren, B. S.-H. Ang, B. S. Yeo, Tuning the selectivity of carbon dioxide electroreduction toward ethanol on oxide-derived CuxZn catalysts. *ACS Catal.* **6**, 8239–8247 (2016).
34. T.-T. Zhuang *et al*., Steering post-C–C coupling selectivity enables high efficiency electroreduction of carbon dioxide to multi-carbon alcohols. *Nat. Catal.* **1**, 421–428 (2018).
35. D. Kim, C. S. Kley, Y. Li, P. Yang, Copper nanoparticle ensembles for selective electroreduction of CO_2 to C_2-C_3 products. *Proc. Natl. Acad. Sci. U.S.A.* **114**, 10560–10565 (2017).
36. C. Reller *et al*., Selective electroreduction of CO_2 toward ethylene on nano dendritic copper catalysts at high current density. *Adv. Energy Mater.* **7**, 1602114 (2017).
37. Y.-X. Duan *et al*., Amorphizing of Cu nanoparticles toward highly efficient and robust electrocatalyst for CO_2 reduction to liquid fuels with high faradaic efficiencies. *Adv. Mater.* **30**, e1706194 (2018).
38. A. K. Singh, J. H. Montoya, J. M. Gregoire, K. A. Persson, Robust and synthesizable photocatalysts for CO_2 reduction: A data-driven materials discovery. *Nat. Commun.* **10**, 443 (2019).
39. M. Liu *et al*., Enhanced electrocatalytic CO_2 reduction via field-induced reagent concentration. *Nature* **537**, 382–386 (2016).
40. C.-T. Dinh *et al*., CO_2 electroreduction to ethylene via hydroxide-mediated copper catalysis at an abrupt interface. *Science* **360**, 783–787 (2018).
41. D. R. Appling, *Biochemistry: Concepts and Connections* (Pearson, Boston, 2016).
42. Y. C. Li *et al*., Bipolar membranes inhibit product crossover in CO_2 electrolysis cells. *Adv. Sustain. Syst.* **2**, 1700187 (2018).
43. D. M. Bierschenk, J. R. Wilson, E. Miller, E. Dutton, S. A. Barnett, A proposed method for high efficiency electrical energy storage using solid oxide cells. *ECS Trans.* **35**, 2969–2978 (2011).
44. S. Choi, T. C. Davenport, S. M. Haile, Protonic ceramic electrochemical cells for hydrogen production and electricity generation: Exceptional reversibility, stability, and demonstrated faradaic efficiency. *Energy Environ. Sci.* **12**, 206–215 (2019).
45. P. Lacorre, F. Goutenoire, O. Bohnke, R. Retoux, Y. Laligant, Designing fast oxide-ion conductors based on $La_2Mo_2O_9$. *Nature* **404**, 856–858 (2000).
46. Z. Liu *et al*., Fabrication and modification of solid oxide fuel cell anodes via wet impregnation/infiltration technique. *J. Power Sources* **237**, 243–259 (2013).
47. X. Yang, J. T. S. Irvine, $(La_{0.75}Sr_{0.25})_{0.95}Mn_{0.5}Cr_{0.5}O_3$ as the cathode of solid oxide electrolysis cells for high temperature hydrogen production from steam. *J. Mater. Chem.* **18**, 2349–2354 (2008).
48. X. Ge, L. Zhang, Y. Fang, J. Zeng, S. Hwa Chan, Robust solid oxide cells for alternate power generation and carbon conversion. *RSC Adv.* **1**, 715–724 (2011).
49. D. J. L. Brett, A. Atkinson, N. P. Brandon, S. J. Skinner, Intermediate temperature solid oxide fuel cells. *Chem. Soc. Rev.* **37**, 1568–1578 (2008).
50. W. Guo, J. Liu, Y. Zhang, Electrical and stability performance of anode-supported solid oxide fuel cells with strontium- and magnesium-doped lanthanum gallate thin electrolyte. *Electrochim. Acta* **53**, 4420–4427 (2008).
51. G. Chiodelli *et al*., Role of synthetic route on the transport properties of $BaCe_{1-x}Y_xO_3$ proton conductor. *J. Alloys Compd.* **470**, 477–485 (2009).
52. K. Katahira, Y. Kohchi, T. Shimura, H. Iwahara, Protonic conduction in Zr-substituted $BaCeO_3$. *Solid State Ion.* **138**, 91–98 (2000).
53. F. He, D. Song, R. Peng, G. Meng, S. Yang, Electrode performance and analysis of reversible solid oxide fuel cells with proton conducting electrolyte of $BaCe_{0.5}Zr_{0.3}Y_{0.2}O_{3-d}$. *J. Power Sources* **195**, 3359–3364 (2010).
54. S. M. Haile, C. R. I. Chisholm, K. Sasaki, D. A. Boysen, T. Uda, Solid acid proton conductors: From laboratory curiosities to fuel cell electrolytes. *Faraday Discuss* **134**, 17–39, discussion 103–118, 415–419 (2007).
55. J. Kim *et al*., Hybrid-solid oxide electrolysis cell: A new strategy for efficient hydrogen production. *Nano Energy* **44**, 121–126 (2018).
56. Haldor Topsøe, "Produce your own CO B'eCOs it's better" (2019). https://info.topsoe.com/ecos. Accessed 9 December 2019.
57. E. Vasileiou *et al*., Electrochemical enhancement of ammonia synthesis in a $BaZr_{0.7}Ce_{0.2}Y_{0.1}O_{2.9}$ solid electrolyte cell. *Solid State Ion.* **288**, 357–362 (2016).
58. J. N. Renner, L. F. Greenlee, K. E. Ayres, A. M. Herring, Electrochemical synthesis of ammonia: A low pressure, low temperature approach. *Electrochem. Soc. Interface* **24**, 51–57 (2015).
59. V. Kyriakou, I. Garagounis, E. Vasileiou, A. Vourros, M. Stoukides, Progress in the electrochemical synthesis of ammonia. *Catal. Today* **286**, 2–13 (2017).
60. T. Murakami, T. Nishikiori, T. Nohira, Y. Ito, Investigation of anodic reaction of electrolytic ammonia synthesis in molten salts under atmospheric pressure. *J. Electrochem. Soc.* **152**, D75–D78 (2005).
61. A. L. Shaula *et al*., Oxygen permeability of mixed-conducting composite membranes: Effects of phase interaction. *J. Solid State Electrochem.* **10**, 28–40 (2006).
62. E. Skúlason *et al*., A theoretical evaluation of possible transition metal electrocatalysts for N_2 reduction. *Phys. Chem. Chem. Phys.* **14**, 1235–1245 (2012).